
EXACT FIXED-RADIUS NEAREST NEIGHBOR SEARCH WITH AN APPLICATION TO CLUSTERING

Xinye Chen

Department of Mathematics
The University of Manchester
Manchester

xinye.chen@manchester.ac.uk

Stefan Güttel

Department of Mathematics
The University of Manchester
Manchester

stefan.guettel@manchester.ac.uk

ABSTRACT

Fixed-radius nearest-neighbor search is a common database operation that retrieves all data points within a user-specified distance to a query point. There are efficient approximate nearest neighbor search algorithms that provide fast query responses but they often have a very compute-intensive indexing phase and require parameter tuning. Therefore, exact brute force and tree-based search methods are still widely used. Here we propose a new fixed-radius nearest neighbor search method that significantly improves over brute force and tree-based methods in terms of index and query time, returns exact results, and requires no parameter tuning. The method exploits a sorting of the data points by their first principal component, thereby facilitating a reduction in query search space. Further speedup is gained from an efficient implementation using high-level Basic Linear Algebra Subprograms (BLAS). We provide theoretical analysis of our method and demonstrate its practical performance when used stand-alone and when applied within a clustering algorithm.

Keywords Nearest neighbor search · Information retrieval and search · Clustering

1 Introduction

The retrieval of nearest neighbors is a fundamental data operation. Given a data point, this operation aims at finding the most similar data points (often stored in a database) using a predefined distance function. Nearest neighbor search has many applications in computer science and machine learning, including object recognition [1, 2], image descriptor matching [3], time series indexing [4, 5, 6], clustering [7, 8, 9, 10, 11], pose estimation [12], computational linguistics [13], and information retrieval [14].

There are two types of nearest neighbor (NN) search: *k-nearest neighbor* and *fixed-radius neighbor* search. Fixed-radius NN search, also referred to as *radius query*, aims at identifying all data points within a given distance from a query point; see [15] for a historical review. The most straightforward way of finding nearest neighbors is via a linear search through the whole database, also known as exhaustive or brute force search. Though considered inelegant, it is still widely used, e.g., in combination with GPU acceleration [16].

Existing NN search approaches can be broadly divided into *exact* and *approximate* methods. It is widely accepted that for high-dimensional data there are no exact NN search methods which are more efficient than exhaustive search; see, e.g., [17, Chap. 3] and [18]. Exact NN methods based on *k-d tree* [19, 20], *balltree* [21], *VP-tree* [22], *cover tree* [23], and *RP tree* [24] only perform well on low-dimensional data. This shortcoming is often referred to as the curse of dimensionality [25]; see also [26, 27].

In many applications, approximate methods are an effective solution by seeking fast queries while allowing for a small loss. Well-established approximate NN search techniques include randomized *k-d trees* [3], hierarchical *k-means* [2], locality sensitive hashing [25], HNSW [28], and ScaNN [29]. Considerable drawbacks of most approximate NN search algorithms are their potentially long indexing time and the need for the tuning of additional hyperparameters (such as the trade-off between recall versus index and query time). Furthermore, to the best of our knowledge, all approximate

NN methods for which open-source implementations (such as those referenced in the footnote¹) are available only address the k-nearest neighbor problem, not the fixed-radius search discussed here.

In this paper we introduce a new *exact* approach to fixed-radius NN search based on sorting, referred to as SNN for short. Appealing properties of SNN are

1. simplicity: there are no hyperparameters except for the user-specified search radius
2. exactness: SNN is guaranteed to return all nearest neighbors within the search radius
3. speed: SNN demonstrably outperforms other exact NNS algorithms like, e.g., methods based on tree structures
4. flexibility: the low index time of SNN makes it applicable in an online streaming setting.

The rest of this paper is organized as follows. In section 2, we introduce our sorting-based NN method, detailing its index and query phases. Section 3 contains computational considerations regarding the efficient implementation and behaviour in floating-point arithmetic. Some further theoretical considerations are given in section 4. Section 5 contains an empirical study and comparison of our algorithm to other state-of-the-art NN methods. In section 6 we present an application of our method to clustering problems, and then conclude in section 7.

2 Sorting-based NN search

Suppose we have n data points $p_1, \dots, p_n \in \mathbb{R}^d$ (represented as column vectors) and $d \ll n$. The fixed-radius NN problem consists of finding the subset of data points that is closest to a given query point $q \in \mathbb{R}^d$ (may be out-of-sample) with respect to some distance metric. Throughout this paper, the distance is Euclidean, though it is also possible to identify nearest neighbors with a “smallest angle” criterion. For example, assuming we operate on normalized data (with $\|u\| = \|v\| = 1$), the cosine distance is defined as

$$\text{cdist}(u, v) = 1 - \angle(u, v) = 1 - \frac{u^T v}{\|u\| \|v\|} = 1 - u^T v.$$

The squared Euclidean distance is equivalent to

$$\|u - v\|^2 = 2(1 - \angle(u, v)) = 2\text{cdist}(u, v).$$

Similarly, the deduction can be extended to angular distance. Our algorithm, called SNN, will return the required indices of the nearest neighbors, and can also return the corresponding distances if needed.

SNN uses three essential ingredients to obtain its speed:

- a sorting-based exclusion criterion is used to prune the search space for a given query
- pre-calculated dot products of the data points allow for a reduction of arithmetic complexity, and
- reformulation of the distance criterion in terms of matrices (instead of vectors) allows for the use of high-level BLAS (basic linear algebra subprograms) [30].

In the following, we explain these ingredients in more detail.

2.1 Indexing

Before sorting the data, all data points are centered by subtracting the empirical mean value of each dimension:

$$x_i := p_i - \text{mean}(\{p_j\}).$$

This operation will not affect the pairwise Euclidean distance between the data points and can be performed in $O(dn)$ operations, i.e. with linear complexity in n . We then compute the first principal component $v_1 \in \mathbb{R}^d$, i.e., the vector along which the data $\{x_i\}$ exhibits largest empirical variance. This vector can be computed by a thin singular value decomposition of the tall-skinny data matrix $X := [x_1, \dots, x_n]^T \in \mathbb{R}^{n \times d}$,

$$X = U \Sigma V^T, \tag{1}$$

¹<https://github.com/spotify/annoy>, <https://pynndescent.readthedocs.io/>, <https://github.com/google-research/google-research/tree/master/scann>, <https://github.com/nmslib/hnswlib>

where $U \in \mathbb{R}^{n \times d}$ and $V \in \mathbb{R}^{d \times d}$ have orthonormal columns and $\Sigma = \text{diag}(\sigma_1, \dots, \sigma_d) \in \mathbb{R}^{d \times d}$ is a diagonal matrix such that $\sigma_1 \geq \sigma_2 \geq \dots \geq \sigma_d \geq 0$. The principal components are given as the columns of $V = [v_1, \dots, v_d]$ and we require only the first column v_1 . The score of a point x_i along v_1 is

$$\alpha_i := x_i^T v_1 = (e_i^T X) v_1 = (e_i^T U \Sigma V^T) v_1 = e_i^T u_1 \sigma_1,$$

where e_i denotes the i -th canonical unit vector in \mathbb{R}^n . In other words, the scores α_i of all points can be read off from the first column of $U = [u_1, \dots, u_d]$ times σ_1 . The computation of the scores using a thin SVD requires $O(nd^2)$ operations and is therefore linear in n .

The next (and most important) step is to order all data points x_i by their α_i scores; that is,

$$(x_i) := \text{sort}(\{x_i\})$$

so that $\alpha_1 \leq \alpha_2 \leq \dots \leq \alpha_n$ with each $\alpha_i = x_i^T v_1$. This sorting will generally require a time complexity of $O(n \log n)$ independent of the data dimension d . All these computations are done in an index phase and only the scores $[\alpha_i]$ and the single vector v_1 need to be stored.

The indexing phase is summarized in Algorithm 1.

2.2 Query

Given a query point q and user-specified search radius R , we want to retrieve all data points p_i satisfying $\|q - p_i\| \leq R$. Figure 1 illustrates our approach. We first form the mean-centered query $x_q := q - \text{mean}(\{p_j\})$ and the corresponding score $\alpha_q := x_q^T v_1$. By utilizing the Cauchy-Schwarz inequality, we have

$$|\alpha_i - \alpha_q| = |v_1^T x_i - v_1^T x_q| \leq \|x_i - x_q\|. \quad (2)$$

Since we have sorted the x_i such that $\alpha_1 \leq \alpha_2 \leq \dots \leq \alpha_n$, the following statements are true:

if $\alpha_q - \alpha_{j_1} > R$ for some j_1 , then $\|x_i - x_q\| > R$ for all $i \leq j_1$;

if $\alpha_{j_2} - \alpha_q > R$ for some j_2 , then $\|x_i - x_q\| > R$ for all $i \geq j_2$.

As a consequence, we only need to consider *candidates* x_i whose indices are in $J := \{j_1 + 1, j_1 + 2, \dots, j_2 - 1\}$ and we can determine the smallest such set by finding the largest j_1 and smallest j_2 satisfying the above statements, respectively. As the α_i are sorted, this can be achieved via binary search in $O(\log n)$ operations. Note that the indices in J are continuous integers, and hence it is memory efficient to access $X(J, :)$, the submatrix of X whose row indices are in J . This will be important later.

Finally, we filter all data points in the reduced set $X(J, :)$, retaining only those data points whose distance to the query point x_q is less or equal to R , i.e., points satisfying $\|x_j - x_q\|^2 \leq R^2$. The query phase is summarized in Algorithm 2.

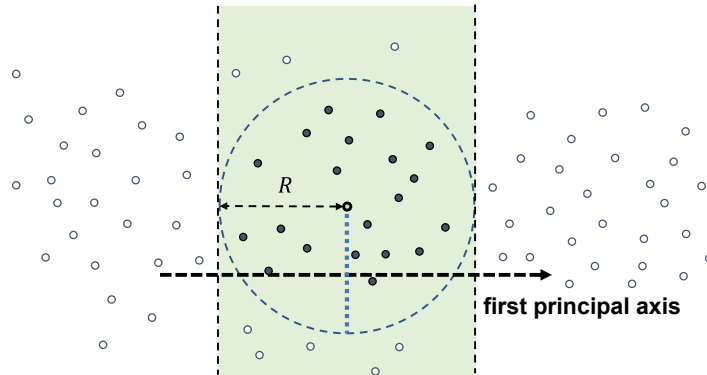


Figure 1: Query with radius R . The data points in the shaded band have their first principal coordinate within a distance R from the first principal coordinate of the query point, and hence are NN candidates. All data points are sorted so that all candidates have continuous indices.

3 Computational considerations

The compute-intensive step of the query procedure is the computation of

$$\|x_j - x_q\|^2 = (x_j - x_q)^T(x_j - x_q) \quad (3)$$

for all vectors x_j with indices $j \in J$. Assuming that these vectors have d features, one evaluation of (3) requires $3d - 1$ floating point operations (flop): d flop for the subtractions, d flop for the squaring, and $d - 1$ flop for the summation. In total, $|J|(3d - 1)$ flop are required to compute all $|J|$ squared distances. We can equivalently rewrite (3) as $\|x_j - x_q\|^2 = x_j^T x_j + x_q^T x_q - 2x_j^T x_q$ and instead verify the radius condition as

$$\frac{1}{2}x_j^T x_j - x_j^T x_q \leq \frac{R^2 - x_q^T x_q}{2}. \quad (4)$$

This form has the advantage that all the inner products $(x_j^T x_j)/2$ ($i = 1, 2, \dots, n$) can be pre-computed during the indexing phase. Hence, in the query phase, the left-hand side of (4) can be evaluated for all $|J|$ points x_j using only $2d|J|$ flop: $(2d - 1)|J|$ for the inner products and $|J|$ subtractions.

Merely counting flop, (4) saves about 1/3 of arithmetic operations over (3). An additional advantage results from the fact that all inner products in (4) can be computed as $X(J, :)^T x_q$ using level-2 BLAS matrix-vector multiplication (`gemv`), resulting in further speedup on modern computing architectures. If multiple query points are given, say $x_q^{(1)}, \dots, x_q^{(\ell)}$, a level-3 BLAS matrix-matrix multiplication (`gemm`) evaluates $X(J, :)^T [x_q^{(1)}, \dots, x_q^{(\ell)}]$ in one go, where J is the union of candidates for all ℓ query points.

One may be concerned that the computation using (4) incurs more rounding error than the usual formula (3). We now show that this is not the case. First, note that division or multiplication by 2 does not incur rounding error. Using the standard model of floating point arithmetic, we have $fl(a \circ b) = (a \circ b)(1 \pm \delta)$ for any elementary operation $\circ \in \{+, -, \times, /\}$, where $0 \leq \delta \leq u$ with the unit roundoff u [31, Chap. 1]. Suppose we have two vectors x and y where x_i and y_i denote their respective coordinates. Then computing

$$s_d := \sum_{i=1}^d (x_i - y_i)^2 = (x - y)^T(x - y)$$

in floating point arithmetic amounts to evaluating

$$\begin{aligned} \hat{s}_1 &= fl((x_1 - y_1)^2) = fl((x_1 - y_1))^2 \cdot (1 \pm \delta) = (x_1 - y_1)^2(1 \pm \delta)^3, \\ \hat{s}_2 &= fl(\hat{s}_1 + (x_2 - y_2)^2) = (\hat{s}_1 + (x_2 - y_2)^2)(1 \pm \delta)^3 \cdot (1 \pm \delta) \\ &= (x_1 - y_1)^2(1 \pm \delta)^4 + (x_2 - y_2)^2(1 \pm \delta)^4, \text{ and so on.} \end{aligned}$$

Continuing this recursion we arrive at

$$\begin{aligned} \hat{s}_d &= (x_1 - y_1)^2(1 \pm \delta)^{d+2} + (x_2 - y_2)^2(1 \pm \delta)^{d+2} \\ &\quad + (x_3 - y_3)^2(1 \pm \delta)^{d+1} + \dots + (x_d - y_d)^2(1 \pm \delta)^4. \end{aligned}$$

Assuming $ju < 1$ and using [31, Lemma 3.1] we have

$$(1 \pm \delta)^j = 1 + \theta_j, \text{ where } |\theta_j| \leq \frac{ju}{1 - ju} := \gamma_j.$$

Hence,

$$\begin{aligned} &|(x - y)^T(x - y) - fl((x - y)^T(x - y))| \\ &\leq |\theta_{d+2}(x_1 - y_1)^2 + \theta'_{d+2}(x_2 - y_2)^2 + \theta_{d+1}(x_3 - y_3)^2 + \dots \\ &\quad + \theta_4(x_d - y_d)^2| \\ &\leq |\theta_{d+2}|(x_1 - y_1)^2 + |\theta'_{d+2}|(x_2 - y_2)^2 + |\theta_{d+1}|(x_3 - y_3)^2 + \dots \\ &\quad + |\theta_4|(x_d - y_d)^2 \\ &\leq \gamma_{d+2}(x - y)^T(x - y), \end{aligned}$$

showing that the left-hand side of (3) can be evaluated with high relative accuracy.

A very similar calculation can be done for the formula

$$x^T x + y^T y - 2x^T y = s_d,$$

the expression that is used to derive (4). Using the standard result for inner products [31, eq. (3.2)]

$$\begin{aligned} fl(x^T y) &= x_1 y_1 (1 \pm \delta)^d + x_2 y_2 (1 \pm \delta)^d + x_3 y_3 (1 \pm \delta)^{d-1} + \dots \\ &\quad + x_d y_d (1 \pm \delta)^2, \end{aligned}$$

one readily derives

$$\begin{aligned} &|(x - y)^T (x - y) - fl(x^T x + y^T y - 2x^T y)| \\ &\leq \gamma_{d+2} (x - y)^T (x - y), \end{aligned}$$

the same bound on the relative accuracy of floating-point evaluation as obtained for (3).

Algorithm 1 Index

- 1: **Input:** Data matrix $P = [p_1, p_2, \dots, p_n]^T \in \mathbb{R}^{n \times d}$
 - 2: Compute $\mu := \text{mean}(\{p_j\})$
 - 3: Compute the mean-centered matrix X with rows $x_i := p_i - \mu$
 - 4: Compute the singular value decomposition of $X = U \Sigma V^T$
 - 5: Compute the sorting keys $\alpha_i = x_i^T v_1$ for $i = 1, 2, \dots, n$
 - 6: Sort data points X such that $\alpha_1 \leq \alpha_2 \leq \dots \leq \alpha_n$
 - 7: Compute $\bar{x}_i = (x_i^T x_i)/2$ for $i = 1, 2, \dots, n$
 - 8: **Return:** $\mu, X, v_1, [\alpha_i], [\bar{x}_i]$
-

Algorithm 2 Query

- 1: **Input:** Query vector q ; user-specified radius R ; output from Algorithm 1
 - 2: Compute $x_q := q - \mu$
 - 3: Compute the sorting score of x_q , i.e., $\alpha_q := x_q^T v_1$
 - 4: Select candidate index range J so that $|\alpha_j - \alpha_q| \leq R$ for all $j \in J$
 - 5: Compute $d := \bar{x}(J) - X(J, :)^T x_q$ using the precomputed $\bar{x} = [\bar{x}_i]$
 - 6: **Return:** Points x_j with $d_j \leq (R^2 - x_q^T x_q)/2$ according to (4)
-

4 Analysis

The efficiency of the query approach described in Algorithm 2 is dependent on the number of pairwise distance computations that are performed in Step 5, depending on the size of the index set $|J|$. If the index set J is the full $\{1, 2, \dots, n\}$, then the algorithm reduces to exhaustive search over the whole dataset, which is undesirable. For the algorithm to be most efficient, $|J|$ would exactly coincide with the indices of data points x_i that satisfy $\|x_i - x_q\| \leq R$. In practice, the index set J will be somewhere in between these two extremes. Thus, it is natural to ask: *How likely is it that $|\alpha_i - \alpha_q| \leq R$, yet $\|x_i - x_q\| > R$?*

First note that, using the singular value decomposition (1) of the data matrix X , we can derive an upper bound on $\|x_i - x_q\|$ that complements the lower bound (2). Using that $x_i^T = e_i^T X = e_i^T U \Sigma V^T$, where $e_i \in \mathbb{R}^n$ denotes the i th canonical unit vector, and denoting the elements of U by u_{ij} , we have

$$\begin{aligned} \|x_i - x_q\|^2 &= |\alpha_i - \alpha_q|^2 + \left\| [(u_{i2} - u_{q2}), \dots, (u_{id} - u_{qd})] \hat{\Sigma} \right\|^2 \leq |\alpha_i - \alpha_q|^2 + \|u_i - u_q\|^2 \cdot \|\hat{\Sigma}\|^2 \\ &\leq |\alpha_i - \alpha_q|^2 + 2\sigma_2^2 \end{aligned}$$

with $\hat{\Sigma} = \begin{bmatrix} \sigma_2 & & \\ & \ddots & \\ & & \sigma_d \end{bmatrix}$.

Therefore,

$$|\alpha_i - \alpha_q|^2 \leq \|x_i - x_q\|^2 \leq |\alpha_i - \alpha_q|^2 + 2\sigma_2^2 \quad (5)$$

and the gap in these inequalities is determined by σ_2 , the second singular value of X . Indeed, if $\sigma_2 = 0$, then all data points x_i lie on a straight line passing through the origin and their distances correspond exactly to the difference in their first principal coordinates. This is a best-case scenario for Algorithm 2 as all candidates $x_j, j \in J$, found in Step 4 are

indeed also nearest neighbors. If, on the other hand, σ_2 is relatively large compared to σ_1 , the gap in the inequalities (5) becomes large and $|\alpha_i - \alpha_q|$ may be a crude overestimation of the distance $\|x_i - x_q\|$.

In order to get a qualitative understanding of how the number of distance computations in Algorithm 2 depends on the various parameters (dimension d , singular values of the data matrix, query radius R , etc.), we consider the following model. Let $\{x_i\}_{i=1}^n$ be a large sample of points whose d components are normally distributed with zero mean and standard deviation $[1, s, \dots, s]$, $s < 1$, respectively. These points describe an elongated ‘‘Gaussian blob’’ in \mathbb{R}^d , with the elongation controlled by s . In the large data limit ($n \rightarrow \infty$) the singular values of the data matrix $X = [x_1, \dots, x_n]^T$ approach $\sqrt{n}, s\sqrt{n}, \dots, s\sqrt{n}$ and the principal components approach the canonical unit vectors e_1, e_2, \dots, e_d . As a consequence, the principal coordinates $\alpha_i = e_1^T x_i$ follow a standard normal distribution, and hence for any $c \in \mathbb{R}$ the probability that $|\alpha_i - c| \leq R$ is given as

$$P_1 = P_1(c, R) = \frac{1}{\sqrt{2\pi}} \int_{c-R}^{c+R} e^{-r^2/2} dr.$$

On the other hand, the probability that $\|x_i - [c, 0, \dots, 0]^T\| \leq R$ is given by

$$\begin{aligned} P_2 &= P_2(c, R, s, d) \\ &= \frac{1}{\sqrt{2\pi}} \int_{c-R}^{c+R} e^{-r^2/2} \cdot F\left(\frac{R^2 - (r-c)^2}{s^2}; d-1\right) dr, \end{aligned} \quad (6)$$

where F denotes the χ^2 cumulative distribution function. In this model we can think of the point $x_q := [c, 0, \dots, 0]^T$ as a query point, and our aim is to identify all data points x_i within a radius R of this query point.

Since $\|x_i - x_q\| \leq R$ implies that $|\alpha_i - c| \leq R$, we have $P_1 \geq P_2$. Hence, the quotient P_2/P_1 can be interpreted as a conditional probability of a point x_i satisfying $\|x_i - x_q\| \leq R$ given that $|e_1^T x_i - c| \leq R$, i.e.,

$$P = P(\|x_i - x_q\| \leq R \mid |e_1^T x_i - c| \leq R) = P_2/P_1.$$

Ideally, we would like this quotient $P = P_2/P_1$ be close to 1, and it is now easy to study the dependence on the various parameters. First note that P_1 does not depend on s nor d , and hence the only effect these two parameters have on P is via the factor $F\left(\frac{R^2 - (r-c)^2}{s^2}; d-1\right)$ in the integrand of P_2 . This term corresponds to the probability that the sum of squares of $d-1$ independent Gaussian random variables with mean zero and standard deviation s is less or equal to $R^2 - (r-c)^2$. Hence, P_2 and therefore P are monotonically decreasing as s or d are increasing. This is consistent with intuition: as s increases, the elongated point cloud $\{x_i\}$ becomes more spherical and hence it gets more difficult to find a direction in which to enumerate (sort) the points naturally. And this problem gets more pronounced in higher dimensions d .

We now show that ‘‘efficiency ratio’’ P converges to 1 as R increases. In other words, the identification of candidate points $x_j, j \in J$, should become *relatively* more efficient as the query radius R increases. (Here *relative* is meant in the sense that candidate points become more likely to be fixed-radius nearest neighbors as R increases. Informally, as $R \rightarrow \infty$, all n data points are candidates and also nearest neighbors and so the efficiency ratio must be 1.) First note that for an arbitrarily small $\epsilon > 0$ there exists a radius $R_1 > 1$ such that $P_1(c, R_1 - 1) > 1 - \epsilon$. Further, there is a $R_2 > 1$ such that

$$F\left(\frac{R_2^2 - (r-c)^2}{s^2}; d-1\right) > 1 - \epsilon \quad \text{for all } r \in [c - R_2 + 1, c + R_2 - 1].$$

To see this, note that the cumulative distribution function F increases monotonically from 0 to 1 as its first argument increases from 0 to ∞ . Hence there exists a value T for which $F(t, d-1) > 1 - \epsilon$ for all $t \geq T$. Now we just need to find R_2 such that

$$\frac{R_2^2 - (r-c)^2}{s^2} \geq T \quad \text{for all } r \in [c - R_2 + 1, c + R_2 - 1].$$

The left-hand side is a quadratic function with roots at $r = c \pm R_2$, symmetric with respect to the maximum at $r = c$. Hence choosing R_2 such that

$$\frac{R_2^2 - ([c + R_2 - 1] - c)^2}{s^2} = T, \quad \text{i.e.,} \quad R_2 = \left(\frac{T s^2 + 1}{2}\right)^{1/2},$$

or any value R_2 larger than that, will be sufficient. Now, setting $R = \max\{R_1, R_2\}$, we have

$$P_2 \geq \frac{1}{\sqrt{2\pi}} \int_{c-R+1}^{c+R-1} e^{-r^2/2} \cdot F\left(\frac{R^2 - (r-c)^2}{s^2}; d-1\right) dr \geq (1 - \epsilon)^2.$$

Hence, both P_1 and P_2 come arbitrarily close to 1 as R increases, and so does their quotient $P = P_2/P_1$.

5 Empirical study

Our experiments are conducted on a compute server with hardware specifications as shown in Table 1. All algorithms run on single thread with the same settings for fair comparison. All reported numerical results are rounded to two significant digits. We only consider algorithms for which stable Cython or Python implementation are freely available. Our SNN algorithm is implemented in native Python, while scikit-learn’s [32] k -d tree and balltree algorithms use Cython for some part of the computation. The code and data to reproduce the experiments in this paper can be downloaded from²

<https://github.com/nla-group/snn>.

Table 1: Hardware specifications

Operation system	Linux Debian 11
Installed RAM	1.5 TB RAM (=1536 GB RAM)
Processor	2x Intel Xeon Silver 4114 2.2G (total 20 cores, 40 threads)

5.1 Radius query on synthetic data

We first compare k -d tree, balltree, and SNN on synthetically generated data to study their dependence on the data size n and the data dimension d . We also include two brute force methods, the one in scikit-learn [32] (denoted as brute force 1) and another one implemented by us (denoted as brute force 2) which exploits BLAS level-2. The leaf size for scikit-learn’s k -d tree and balltree is kept at the default value 40. The data is sampled from the continuous uniform distribution on $[0, 1]^d$ and normalized with z-score standardization (i.e., shift each feature to zero mean and scale it to unit variance).

For the size test we vary n from 3,000 to 30,000 in increments of 3,000. The data dimension d is chosen from $\{2, 50\}$ and for each d four different radius parameters R as shown in Table 2 are selected. The different radius parameters R are chosen to obtain a good order-of-magnitude variation in the average number of returned data points, denoted as \bar{v} , simulating different use NN use cases with small to large query returns. Also, considering that the sampling density is proportional to $n^{1/d}$ [33, Sec. 2.5], the query radius needs to be adapted to the dimension in order to obtain a meaningful query. The index and query timings are then averaged and plotted in Figure 2 (top). In all cases, SNN has a significantly lower index and query time than the tree-based methods and a lower query time than the two brute force NN methods.

In the second test we vary the data dimension d from 2 to 272 in increments of 30, while keeping the data size fixed at $n = 10,000$. The average number of returned data points \bar{v} shows a good variation as the radius parameter is increased as in Table 2. The average index and query times reported in Figure 2 (bottom) again indicate that SNN is the fastest methods for all considered dimensions, except for the low-dimensional case of $d = 2$ where ball tree has a slightly faster query time.

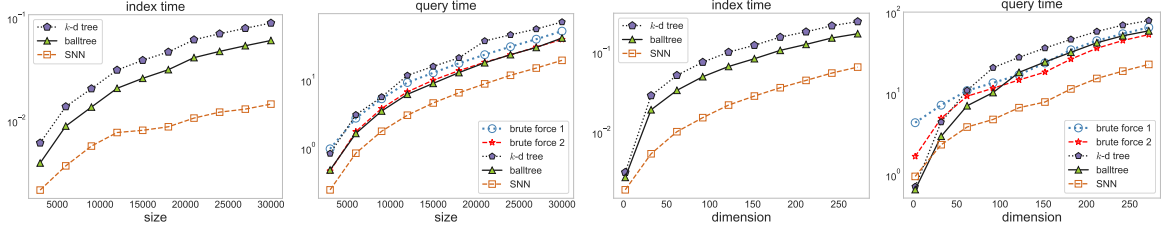
Table 2: Query radius and the number of returned NN averaged over all queries.

Size	$d = 2$	R	0.1	0.3	0.5	0.7
		\bar{v}	54	460	1,200	2,200
	$d = 50$	R	8	10	12	14
		\bar{v}	210	11,000	21,000	21,000
Dimension	$n = 10,000$	R	2.5	9	15.5	22
		\bar{v}	390	1,900	4,500	8,500

5.2 Radius query on real-world data

We now compare the NN search methods on real-world datasets: Fashion-MNIST [34] (images of digits, 60K 784-dimensional points associated with a label from 10 classes, abbreviated as F-MNIST), SIFT [35] (image descriptors,

²All SNN software will be made publicly available on GitHub after the double-blind review.

Figure 2: Index and query time on synthetic data, all in seconds, as the data size n and the dimension d is varied.

two datasets denoted as SIFT10K and SIFT1M for 25,000 and 100,000 of 128-dimensional points), and GIST [36] (image descriptors, 1M of 960-dimensional points). These sets are widely used in approximate NN search benchmarks. The query sets are out-of-sample from the index set: for Fashion-MNIST, SIFT and GIST there are 10,000, 100, 10000, 1000 queries to perform, respectively.

Table 3: Query radius and the number of returned nearest neighbors for synthetic data averaged over all queries.

Dataset	R				
	10	12	14	16	18
F-MNIST	9.3	39	130	340	800
SIFT10K	350	2,000	6,100	11,000	20,000
SIFT1M	1,300	7,700	24,000	45,000	82,000
GIST	42	180	470	930	1,700

We preprocess data with z-score standardization and vary the query radius $R \in \{10, 12, 14, 16, 18\}$. These radii have been chosen to obtain a good order-of-magnitude variation in the number of nearest neighbors as shown in Table 3, assessing the algorithms over a range of possible scenarios from small to large query returns.

According to the timings in Table 4 and Table 5, SNN achieves significant speed-up of the index phase over the two tree-based methods, and a significant reduction in average query time over the tree-based and brute force methods.

Table 4: Index time in seconds for real-world data.

Dataset	Algorithm		
	k -d tree	balltree	SNN
F-MNIST	7.5	5.7	1.1
SIFT10K	0.46	0.37	0.035
SIFT1M	2.8	2.3	0.16
GIST	310	270	25

6 SNN-based Clustering

Many clustering algorithms rely on NN search. For example, the original DBSCAN method [7] uses an R* tree data structure to perform range queries, and the performance of DBSCAN relies crucially on the efficient implementation of such a tree structure [37]. Other trees can be used as well, e.g., k -d tree or balltree. Similarly, the hierarchical density clustering algorithm HDBSCAN [8] also relies on such data structures for its NN search.

Here we propose a clustering algorithm that fully leverages the efficiency of SNN, performing with linear space complexity and near-linear time complexity on a wide range of problems. SNN-based clustering contains two phases, namely, aggregation and merging. We explain these phases in the next two sections, followed by a number of tests.

6.1 Aggregation phase

The aim of the aggregation phase in SNN-based clustering is to group nearby data points together in a computationally inexpensive manner, where “nearby” is simply defined in terms of the Euclidean distance $\|x_i - x_j\|$. As before, we assume the data points $\{x_i\}$ to be mean centered. We consider two data points x_i and x_j close if

$$\|x_i - x_j\| \leq \text{radius} \cdot \text{mext} =: R.$$

Table 5: Average query time in seconds for real-world data.

Dataset \ Algorithm	brute force 1	brute force 2	k-d tree	balltree	SNN
F-MNIST	1,900	500	1,400	910	100
SIFT10K	1.0	0.22	1.4	0.94	0.11
SIFT1M	460	160	590	400	72
GIST	6,100	1,000	2,700	1,900	220

Here, `radius` is a user-chosen tolerance and `mext` is the median extend estimated from the mean-centered data, that is, $\text{mext} = \text{median}(\|x_j\|)$; this ensures the method becomes scale independent.

The greedy aggregation now proceeds as follows: starting with the first data point x_1 (i.e., the one with the smallest α_i value), we assign the data points x_j for $j = 2, 3, \dots$ to the same group G_1 if $\|x_1 - x_j\| \leq R$. This assignment is done by an SNN range query around x_1 with radius R . The point x_1 is also referred to as the *starting point* of group G_1 .

Once the first group G_1 is formed, the assignment process continues with the first data point x_i that is not part of G_1 . This point x_i will be the starting point of the next group G_2 . (We emphasize that the starting points do not need to be searched for; they are always the first data point that was skipped when forming the previous group.) This process continues until all points are assigned to a group.

A pseudocode of the SNN-based aggregation algorithm is given in Algorithm 3. Once completed, all n data points have been partitioned into groups G_1, \dots, G_ℓ with their corresponding starting points $x_{s(1)}, \dots, x_{s(\ell)}$.

Algorithm 3 Aggregation

- 1: **Input:** Data $P = [p_1, p_2, \dots, p_n]^T \in \mathbb{R}^{n \times d}$; user-specified radius R
 - 2: $X, [\alpha_i]$ as returned by Algorithm 1
 - 3: Label all sorted data points x_i as “unassigned”
 - 4: Set $i = 1$ and select x_1 as starting point of the first group
 - 5: Obtain set of nearest neighbors $\mathcal{Q}(x_i, R)$ via SNN query (Algorithm 2).
 - 6: Assign $\mathcal{Q}(x_i, R)$ to the same group as x_i .
 - 7: Select the first unassigned point x_i as the next starting point. Repeat steps 5–7 until there are no unassigned points left.
 - 8: **Return:** Assigned points x_1, x_2, \dots, x_n .
-

6.2 Merging on starting points

The second phase of the SNN-based clustering method merges the groups G_1, \dots, G_ℓ into clusters $C_1, \dots, C_k, k \leq \ell$. The merging is done based on distances between the starting points $x_{s(1)}, \dots, x_{s(\ell)}$ as follows: we construct an undirected nearest neighbor graph by connecting two starting points $x_{s(i)}, x_{s(j)}$ if and only if

$$\|x_{s(i)} - x_{s(j)}\| \leq \text{scale} \cdot R, \quad (7)$$

where `scale` is a tuning parameter in the interval $[1, 2]$, which can be set to `scale` = 1.5 in most cases. (To motivate this, note that two distinct starting points $x_{s(i)}$ and $x_{s(j)}$ will never have a distance less than R , as otherwise they would have ended up in the same group G_i during aggregation. Also, if two starting points have a distance greater than $2R$, their surrounding R -balls have no overlap.) The pairing of starting points, required to form the graph, can again be done by using SNN queries.

Once the nearest neighbor graph is formed, we compute its connected components using depth-first search [38] or a disjoint-set data structure [39]. The complexity of this procedure is $O(\max(\ell, E))$, where E is the number of edges in the graph. All data points x_i which are not starting points are naturally assigned to the same cluster as the starting point of the group they belong to. See also Algorithm 4.

Finally, we briefly mention that the merging procedure can be easily altered to identify or reallocate “outliers”, i.e., data points in clusters with only a small number of elements. Defining a minimum cluster size `minPts`, we simply re-allocate outliers to a closest group that has been assigned to a cluster with at least `minPts` points. This can be done by using the starting points alone. For out-of-sample data we employ the same group assignment procedure as for outliers.

Algorithm 4 Group merging

-
- 1: **Input:** Starting points $x_{s(1)}, x_{s(2)}, \dots, x_{s(\ell)}$; user-specified radius R .
 - 2: Construct NN graph with starting points as vertices using Algorithm 2.
 - 3: Find connected components in the graph.
 - 4: Assign the data to the components associated with the starting points.
 - 5: **Return:** Connected graph components.
-

6.3 Test: Scikit-learn clustering benchmark

We now compare our SNN-based clustering algorithm with mean shift [40, 41], DBSCAN [7], HDBSCAN [8], and Quickshift++ [42] (an extension of Quickshift [43]) on the scikit-learn clustering benchmark.³ The library provides preset parameters for mean shift and DBSCAN and we have left them unchanged. We added HDBSCAN, Quickshift++, and SNN-based clustering to the benchmark and tuned the methods by hyperparameter grid search for a best adjusted Rand index (ARI) and adjusted mutual information (AMI) score. The achieved scores are listed in Table 6.

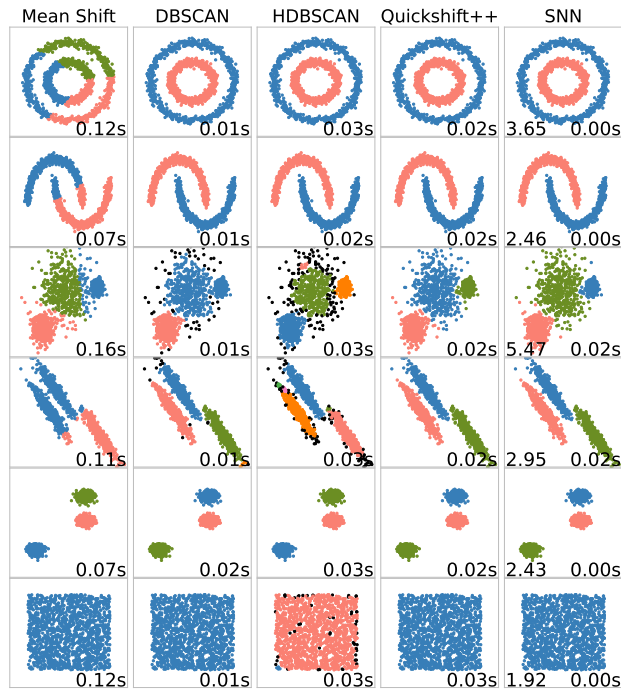


Figure 3: Scikit-learn clustering benchmark. The computation time is shown on the bottom right. For SNN the average number of distance computations per data point is shown on the bottom left.

The visual clustering results are shown in Figure 3 together with the runtime on the bottom right of each plot (all timings are averages of 10 repeated runs). We also show the average number of Euclidean distance computations per data point for SNN in the bottom left. On these six datasets, all methods except mean shift produce good clusters. All methods can be considered fast, with just a few milliseconds of runtime, but SNN is consistently among the fastest methods. This is explained by the small average number of distance computations per data point that are required, never exceeding 5.47 comparisons per data point for any of the tests.

6.4 Test: Image segmentation

Image segmentation is the task of partitioning an image into homogeneous regions according to visual appearance or displayed objects. Here we apply our SNN-based clustering method to segment images from ImageNet [44]. The clustering is employed on a pixel-by-pixel level, treating each pixel in the image as a separate data point. The clearer and more structured the image reconstructed from the segments (clusters) is, the better the segmentation.

³<https://scikit-learn.org/stable/modules/clustering.html>

Table 6: Achieved scores for the scikit-learn clustering benchmark. Datasets I–VI correspond to the row numbers in Figure 3. The ARI and AMI scores are shown on the top and bottom of each cell, respectively.

Dataset	Mean Shift	DBSCAN	HDBSCAN	Quickshift++	SNN
I	0.01 0.01	1.00 1.00	1.00 1.00	1.00 1.00	1.00 1.00
II	0.55 0.44	1.00 1.00	1.00 1.00	1.00 1.00	1.00 1.00
III	0.84 0.83	0.55 0.66	0.86 0.84	0.94 0.92	0.95 0.92
IV	0.53 0.63	0.97 0.95	0.89 0.86	1.00 1.00	1.00 1.00
V	1.00 1.00	1.00 1.00	1.00 1.00	1.00 1.00	1.00 1.00
VI	1.00 1.00	1.00 1.00	0.00 0.00	1.00 1.00	1.00 1.00

According to the visual results in Figure 4, most of the competing algorithms cannot recover images clearly while SNN consistently produces good results. Note that we have tried to tune all methods such that the number of clusters (segments) is roughly comparable. In terms of runtime, shown in the bottom right of each image, SNN is significantly faster than its competitors for five of the six problems and always among the two fastest methods. Again, this is explained by the relatively small average number of distance computations per data point shown in the bottom left of each SNN image.

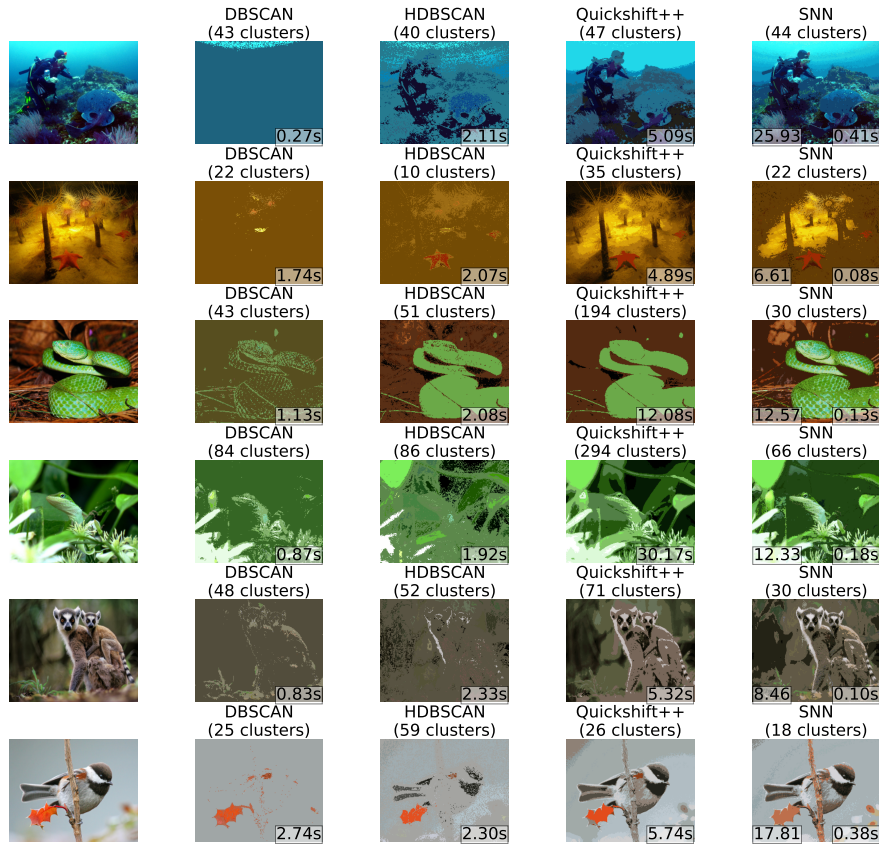


Figure 4: Image segmentation via clustering. We show the runtime on the bottom right of each image and the average number of distance computations per data point on the bottom left of the SNN images.

7 Conclusions

We presented a fast fixed-radius nearest neighbor search method called SNN. Compared to other exact NN search approaches such as k -d tree and balltree, SNN enjoys faster index and query time, which is certainly desirable in a wide range of applications. SNN outperforms different implementations of brute force search. Just like brute force search, SNN requires no parameter tuning and is hence straightforward to use. We also introduced a two-phase distance-based clustering method based on SNN and demonstrated its effectiveness on a range of datasets.

Acknowledgements. Stefan Güttel acknowledges a fellowship from The Alan Turing Institute under the EPSRC grant EP/W001381/1.

References

- [1] James Philbin, Ondrej Chum, Michael Isard, Josef Sivic, and Andrew Zisserman. Object retrieval with large vocabularies and fast spatial matching. In *IEEE Conference on Computer Vision and Pattern Recognition*, pages 1–8, 2007.
- [2] David Nister and Henrik Stewenius. Scalable recognition with a vocabulary tree. In *IEEE Computer Society Conference on Computer Vision and Pattern Recognition (CVPR’06)*, volume 2, pages 2161–2168, 2006.
- [3] Chanop Silpa-Anan and Richard Hartley. Optimised kd-trees for fast image descriptor matching. In *IEEE Conference on Computer Vision and Pattern Recognition*, pages 1–8, 2008.
- [4] Eamonn Keogh and Chotirat Ann Ratanamahatana. Exact indexing of dynamic time warping. *Knowledge and information systems*, 7(3), 2005.
- [5] Kaushik Chakrabarti, Eamonn Keogh, Sharad Mehrotra, and Michael Pazzani. Locally adaptive dimensionality reduction for indexing large time series databases. *ACM Transactions on Database Systems*, 27(2):188–228, 2002.
- [6] Djamel-Edine Yagoubi, Reza Akbarinia, Florent Massegli, and Themis Palpanas. Massively distributed time series indexing and querying. *IEEE Transactions on Knowledge and Data Engineering*, 32(1):108–120, 2020.
- [7] Martin Ester, Hans-Peter Kriegel, Jörg Sander, and Xiaowei Xu. A density-based algorithm for discovering clusters in large spatial databases with noise. In *Proceedings of the Second International Conference on Knowledge Discovery and Data Mining*, KDD’96, pages 226–231. AAAI Press, 1996.
- [8] Ricardo J. G. B. Campello, Davoud Moulavi, and Joerg Sander. Density-based clustering based on hierarchical density estimates. In *Advances in Knowledge Discovery and Data Mining*, pages 160–172. Springer, 2013.
- [9] Antonio-Javier Gallego, Jorge Calvo-Zaragoza, Jose J. Valero-Mas, and Juan R. Rico-Juan. Clustering-based k -nearest neighbor classification for large-scale data with neural codes representation. *Pattern Recognition*, 74:531–543, 2018.
- [10] Mashaan Alshammari, John Stavrakakis, and Masahiro Takatsuka. Refining a k -nearest neighbor graph for a computationally efficient spectral clustering. *Pattern Recognition*, 114:107869, 2021.
- [11] Antonio Javier Gallego, Juan Ramón Rico-Juan, and Jose J. Valero-Mas. Efficient k -nearest neighbor search based on clustering and adaptive k values. *Pattern Recognition*, 122:108356, 2022.
- [12] Shakhnarovich, Viola, and Darrell. Fast pose estimation with parameter-sensitive hashing. In *Proceedings Ninth IEEE International Conference on Computer Vision*, volume 2, pages 750–757, 2003.
- [13] Olha Kaminska, Chris Cornelis, and Veronique Hoste. Nearest neighbour approaches for emotion detection in tweets. In *Proceedings of the Eleventh Workshop on Computational Approaches to Subjectivity, Sentiment and Social Media Analysis*, pages 203–212. Association for Computational Linguistics, 2021.
- [14] Xiubo Geng, Tie-Yan Liu, Tao Qin, Andrew Arnold, Hang Li, and Heung-Yeung Shum. Query dependent ranking using k -nearest neighbor. In *Proceedings of the 31st Annual International ACM SIGIR Conference on Research and Development in Information Retrieval*, SIGIR ’08, pages 115–122. ACM, 2008.
- [15] Jon L Bentley. A survey of techniques for fixed radius near neighbor searching. Technical report, 1975.
- [16] Vincent Garcia, Eric Debreuve, and Michel Barlaud. Fast k nearest neighbor search using GPU. In *IEEE Computer Society Conference on Computer Vision and Pattern Recognition Workshops*, pages 1–6, 2008.
- [17] Marius Muja. *Scalable nearest neighbour methods for high dimensional data*. PhD thesis, University of British Columbia, 2013.
- [18] Matthew Francis-Landau and Benjamin Van Durme. Exact and/or fast nearest neighbors, 2019.

- [19] Jon Louis Bentley. Multidimensional binary search trees used for associative searching. *Communications of the ACM*, 18(9):509–517, 1975.
- [20] Jerome H. Friedman, Jon Louis Bentley, and Raphael Ari Finkel. An algorithm for finding best matches in logarithmic expected time. *ACM Transactions on Mathematical Software*, 3(3):209–226, 1977.
- [21] Stepphen M. Omohundro. Five balltree construction algorithms. Technical report, International Computer Science Institute, 1989.
- [22] Peter N. Yianilos. Data structures and algorithms for nearest neighbor search in general metric spaces. In *Proceedings of the Fourth Annual ACM-SIAM Symposium on Discrete Algorithms*, SODA ’93, pages 311–321. SIAM, 1993.
- [23] Alina Beygelzimer, Sham Kakade, and John Langford. Cover trees for nearest neighbor. In *Proceedings of the 23rd International Conference on Machine Learning*, ICML ’06, pages 97–104. ACM, 2006.
- [24] Sanjoy Dasgupta and Kaushik Sinha. Randomized partition trees for exact nearest neighbor search. In *Proceedings of the 26th Annual Conference on Learning Theory*, volume 30 of *Proceedings of Machine Learning Research*, pages 317–337. PMLR, 2013.
- [25] Piotr Indyk and Rajeev Motwani. Approximate nearest neighbors: towards removing the curse of dimensionality. In *Proceedings of the Thirtieth Annual ACM Symposium on Theory of Computing*, STOC ’98, pages 604–613. ACM, 1998.
- [26] Kevin Beyer, Jonathan Goldstein, Raghu Ramakrishnan, and Uri Shaft. When is “nearest neighbor” meaningful? In *Database Theory — ICDT’99*, pages 217–235. Springer, 1999.
- [27] Christian Böhm, Stefan Berchtold, and Daniel A. Keim. Searching in high-dimensional spaces: index structures for improving the performance of multimedia databases. *ACM Computing Surveys*, 33(3):322–373, 2001.
- [28] Yu A. Malkov and D. A. Yashunin. Efficient and robust approximate nearest neighbor search using hierarchical navigable small world graphs. *IEEE Transactions on Pattern Analysis and Machine Intelligence*, 42(4):824–836, 2020.
- [29] Ruiqi Guo, Philip Sun, Erik Lindgren, Quan Geng, David Simcha, Felix Chern, and Sanjiv Kumar. Accelerating large-scale inference with anisotropic vector quantization. In *Proceedings of the 37th International Conference on Machine Learning*, volume 119 of *Proceedings of Machine Learning Research*, pages 3887–3896. PMLR, 2020.
- [30] L Susan Blackford, Antoine Petitet, Roldan Pozo, Karin Remington, R Clint Whaley, James Demmel, Jack Dongarra, Iain Duff, Sven Hammarling, Greg Henry, et al. An updated set of basic linear algebra subprograms (BLAS). *ACM Transactions on Mathematical Software*, 28(2):135–151, 2002.
- [31] Nicholas J. Higham. *Accuracy and Stability of Numerical Algorithms*. SIAM, 2 edition, 2002.
- [32] F. Pedregosa, G. Varoquaux, A. Gramfort, V. Michel, B. Thirion, O. Grisel, M. Blondel, P. Prettenhofer, R. Weiss, V. Dubourg, J. Vanderplas, A. Passos, D. Cournapeau, M. Brucher, M. Perrot, and E. Duchesnay. Scikit-learn: machine learning in Python. *Journal of Machine Learning Research*, 12:2825–2830, 2011.
- [33] Trevor Hastie, Robert Tibshirani, and Jerome Friedman. *The Elements of Statistical Learning: Data Mining, Inference, and Prediction*. Springer, 2 edition, 2009.
- [34] Han Xiao, Kashif Rasul, and Roland Vollgraf. Fashion-MNIST: a novel image dataset for benchmarking machine learning algorithms, 2017.
- [35] David G. Lowe. Distinctive image features from scale-invariant keypoints. *International Journal of Computer Vision*, 60(2):91–110, 2004.
- [36] Aude Oliva and Antonio Torralba. Modeling the shape of the scene: a holistic representation of the spatial envelope. *International Journal of Computer Vision*, 42:145–175, 2004.
- [37] Hans-Peter Kriegel, Erich Schubert, and Arthur Zimek. The (black) art of runtime evaluation: Are we comparing algorithms or implementations? *Knowledge and Information Systems*, 52:341–378, 2017.
- [38] John Hopcroft and Robert Tarjan. Algorithm 447: efficient algorithms for graph manipulation. *Communications of the ACM*, 16:372–378, 1973.
- [39] Bernard A. Galler and Michael J. Fisher. An improved equivalence algorithm. *Communications of the ACM*, 7:301–303, 1964.
- [40] Yizong Cheng. Mean shift, mode seeking, and clustering. *Transactions on Pattern Analysis and Machine Intelligence*, 17:790–799, 1995.
- [41] Dorin Comaniciu and Peter Meer. Mean shift: a robust approach toward feature space analysis. *Transactions on Pattern Analysis and Machine Intelligence*, 24:603–619, 2002.

- [42] Heinrich Jiang, Jennifer Jang, and Samory Kpotufe. Quickshift++: provably good initializations for sample-based mean shift. In *Proceedings of the 35th International Conference on Machine Learning*, volume 80 of *Proceedings of Machine Learning Research*, pages 2294–2303. PMLR, 2018.
- [43] Andrea Vedaldi and Stefano Soatto. Quick shift and kernel methods for mode seeking. In *European Conference on Computer Vision*, pages 705–718, 2008.
- [44] Jia Deng, Wei Dong, Richard Socher, Li-Jia Li, Kai Li, and Li Fei-Fei. ImageNet: A large-scale hierarchical image database. In *IEEE Conference on Computer Vision and Pattern Recognition*, pages 248–255, 2009.